**Citation**
Pham, T.M. and Le, T.D. and Hao, H. 2019. Flexural performance of precast segmental concrete beams prestressed with CFRP tendons. In Proceedings of 16th East Asian-Pacific Conference on Structural Engineering and Construction (EASEC16), 3-6 Dec 2019. Brisbane, Australia.

16th East Asia-Pacific Conference on Structural Engineering & Construction (EASEC16)
Edited by C.M. Wang, V. Dao and S. Kitipornchai
Brisbane, Australia, December 3-6, 2019

# FLEXURAL PERFORMANCE OF PRECAST SEGMENTAL CONCRETE BEAMS PRESTRESSED WITH CFRP TENDONS

**T.M. PHAM*, T.D. LE and H. HAO**

1Center for Infrastructural Monitoring and Protection, School of Civil and Mechanical Engineering, Curtin University, Kent Street, Bentley, WA 6102, Australia
Emails: thong.pham@curtin.edu.au, tan.le1@postgrad.curtin.edu.au, hong.hao@curtin.edu.au
*Corresponding author

**Abstract**. *This paper presents a part of an ongoing research project on precast segmental concrete beams (PSBs) prestressed with Carbon fibre reinforced polymer (CFRP) tendons, which is currently being conducted at Curtin University. To the authors' best knowledge, this is the first time CFRP tendons were used for segmental concrete beams for the possible replacement of steel tendons to mitigate corrosion-induced damage in the steel tendons at joint locations. Four large-scale segmental concrete beams prestressed with CFRP tendons and one prestressed with steel tendons were tested under four-point loading in the experimental program. The tested results indicated that CFRP tendons can satisfactorily replace the steel tendons for the use in PSBs. All the tested beams exhibited excellent load-carrying and deflection capacities. Bonding condition of the tendons greatly affected the flexural performance of the beams while joint type had a slight effect on the overall performance of the structures. This paper also presents for the first time a numerical approach using Abaqus finite element software to predict the flexural behaviour of segmental concrete beams prestressed with unbonded tendons. The numerical results were validated with experimental results and therefore can be used for design and analysis of the structures.*

**Keywords**: *Segmental concrete beams; Unbonded tendons; Fiber reinforced polymer (FRP) tendons; Numerical analysis; Abaqus*

## 1. INTRODUCTION

Precast segmental prestressed concrete beams (PSBs) have been widely used in bridge construction projects thanks to their time-saving and economic benefits (Le et al. 2018). So far steel tendons have been using as the only a prestressing mean to join individual segments of the structure. Inappropriate design choices and poor quality construction of anti-corrosion systems, however, caused major damage to the structures and in extreme cases, the whole structure was even completely collapsed as reported in the literature (Concrete Society Technical Report 2002). This made corrosion problems of the steel tendons at segment joints a great concern to PSBs, especially in the case the structure is in a very exposed position.

This study investigate the use of fiber-reinforced polymer (FRP) tendons on PSBs as an alternative solution for steel tendons to tackle the corrosion-induced damages on the structure. FRP tendon is corrosion free, high tensile strength and lighter than steel, which allows easier handling and reduces dead load of the structure. The use of FRP tendon on monolithic concrete beams has been extensively reported, however, its application on PSBs has not been reported yet. It is worth noting that FRP tendons show linear stress-strain relationship up to failure, lower

elastic modulus and are weak in shear as compared to steel tendons. It is therefore important to investigate the behavior of PSBs prestressed with FRP tendons before its possible practical applications.

This study also presents a numerical approach to simulate the flexural behavior of PSBs with unbonded tendons using ABAQUS CAE (2012) commercial software. To the authors' best knowledge, this is the first time three-dimensional solid finite elements are used in the numerical model that provides visual observations for better understandings of the flexural behaviour of the structure under the applied loads.

## 2. EXPERIMENTAL PROGRAM

### 2.1. Specimen Design

Four large-scale segmental beams with internal unbonded CFRP tendons and one segmental beams with internal unbonded steel tendons were fabricated and tested in this study. All the beams had T-shape cross-section of 400 mm height and 3.9 m overall length. Each beam consisted of four segments which were made of reinforced concrete ranging from 800 mm to 1150 mm length (Fig. 1). The segments in each beam were joined together by two steel or CFRP tendons, which were internally unbonded or bonded to the concrete using the post-tensioning technique. Table 1 gives details of the beams' configuration.

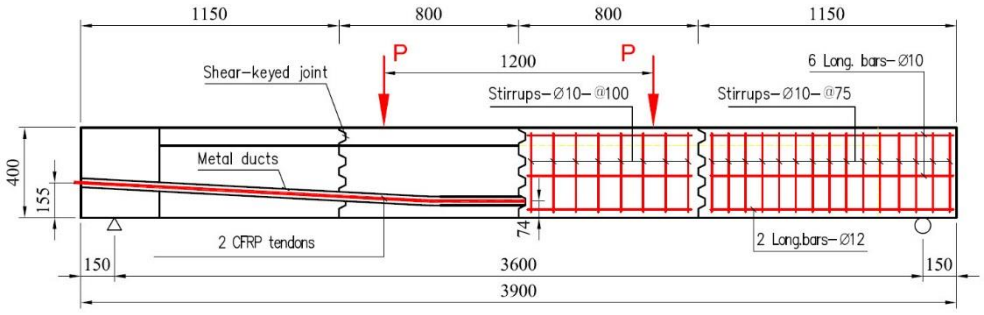


Figure 1. Beams' dimensions and reinforcement.

Table 1. Configuration of tested beams

| Beam | Tendon type | Bonding type | Joint type | $f'_c$ (MPa) | $f_{pe}$ (MPa) | $f_{pe}/f_{pu}$ |
|---|---|---|---|---|---|---|
| BS1 | Steel | Unbonded | Dry | 44 | 1280 | 0.69 |
| BC1 | CFRP | Unbonded | Dry | 44 | 818 | 0.33 |
| BC2 | CFRP | Unbonded | Epoxied | 44 | 661 | 0.27 |
| BC3 | CFRP | Bonded | Dry | 44 | 917 | 0.37 |
| BC4 | CFRP | Bonded | Epoxied | 44 | 942 | 0.38 |

Two 12-mm diameter deformed bars were used for the longitudinal bars at the bottom layer while 10-mm diameter deformed bars were for the top layer. These steel bars were cut-off at the joint locations. 10-mm diameter deformed bars were used for the transverse reinforcements, which were placed at 100-mm spacing for the two middle segments and at 75-mm spacing for the two end segments to strengthen beams in shear.

### 2.2 Materials

The concrete average compressive strength on the testing day was 44 MPa. The ultimate tensile strength of 12-mm deformed bars N12 and 10-mm deformed bars N10 were 587 MPa

and 538 MPa, respectively, as provided by the manufacturer. 12.7-mm diameter steel tendons and single strand 12.9-mm diameter CFRP tendons were used in the specimens. The nominal area, ultimate tensile strength and elastic modulus of the steel tendons were 100 mm2, 1860 MPa, and 195 GPa and those values for CFRP tendons were 126.7 $mm^2$, 2450 MPa and 145 GPa, respectively. More details on the material properties and beams' configuration are found elsewhere (Le et al. 2018; Le et al. 2019).

### 2.3. Fabrication and Test Setup

The segments were cast using match-casting. The joint surfaces and holes of each segment were carefully cleaned before the application of epoxy and grout. Sikadur-30 was used for joining epoxied joints and SikaGrout-300PT was used for creating bonded tendons.

Fig. 2 shows a typical test setup. The applied load was generated by two vertical hydraulic jacks, which were placed equally at one-third span. Load cells were used to monitor the applied load generated by the hydraulic jacks and the force in the tendons. Linear variable differential transformers (LVDTs) were used to measure the beams' deflection and opening of joints. All the beams were cyclically tested under four-point loading test up to failure. All the tests were conducted under the load control at a rate of approximately 3 to 5 kN/min.

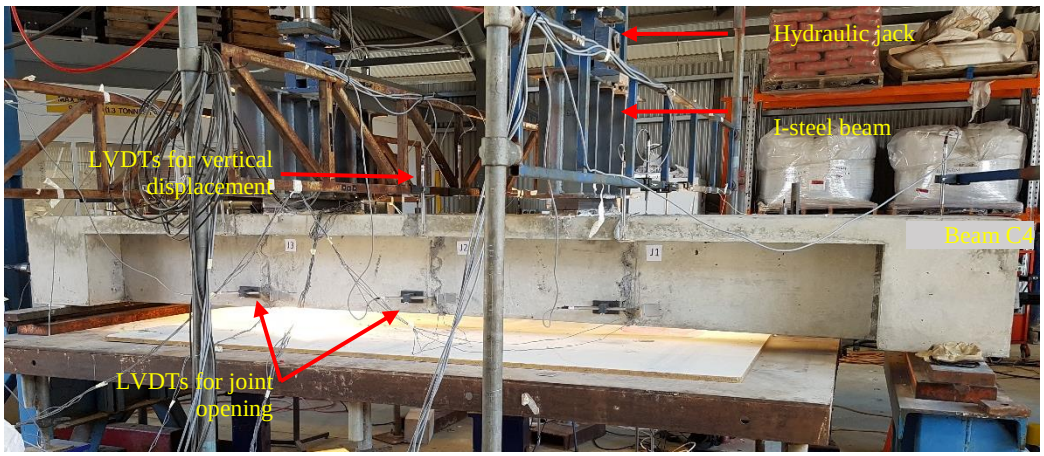


Figure 2. A typical test setup.

## 3. RESULTS AND DISCUSSION

### 3.1. Summary of Tested Results

The envelop load-deflection curves for all the beams under the applied load are shown in Fig. 3. Two stages can be identified for the load-deflection curve of each beam. In the first stage, both beams had high stiffness and exhibited a linear relationship between the applied load and deflection. In the second stage, the beams' stiffness considerably reduced and the beams deformed in a non-linear manner up to failure. The transition from the first stage to the second stage is related to the opening of the middle joint J2 under the applied load. The only difference is that the load-deflection curve of Beam BS1 showed more non-linear behaviour in the second stage compared to the curves of the other beams especially after the yielding of the steel tendons. Table 2 gives the tested results of all the beams, in which $P_u$, $\delta_{mid,u}$ and $\Delta_{J,u}$ are the applied load, midspan deflection, and opening of the middle joint of the specimens at the ultimate stage, respectively.

Photos of the specimens' failures are presented in Fig. 5, which clearly show different failure modes of the tested beams. Beams BS1 failed by the yielding of steel tendons and then the top concrete crushed when the beams underwent large deflection. Beam BC1 and BC2 with

unbonded CFRP tendons failed by concrete spalling on the compressive zone and CFRP tendons rupturing. The crushing of concrete and rupturing of tendons occurred at the middle joint at the midspan for all the specimens. In contrast, Beams BC3 and BC4 with bonded tendons failed by the rupture of CFRP tendons without any concrete spalling on the top.

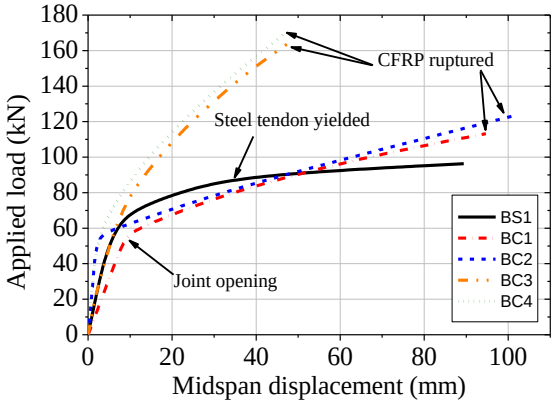


Figure 3. Load-deflection curves

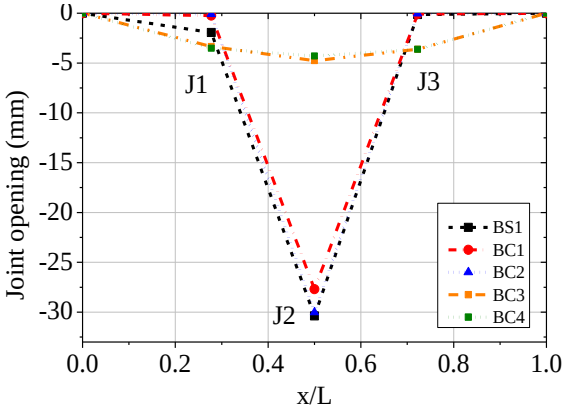


Figure 4. Openings of joints

| Beam | $P_u$ | $\delta_{mid,u}$ | $\Delta_{J,u}$ | Failure mode |
|---|---|---|---|---|
| BS1 | 96 | 89.4 | 30.4 | Yielding of steel tendons and top concrete crushed |
| BC1 | 113 | 94.7 | 27.7 | Top concrete crushed and CFRP tendons ruptured |
| BC2 | 123 | 101.1 | 30.0 | Top concrete crushed and CFRP tendons ruptured |
| BC3 | 164 | 47.8 | 4.7 | CFRP tendons ruptured |
| BC4 | 169 | 46.6 | 3.5 | CFRP tendons ruptured |

Table 2. Tested results of all beams


a) BS1


b) BC1

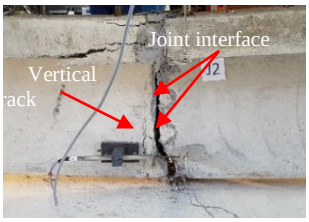


c) BC2


d) BC3


e) BC4

Figure 5. Failure modes of tested beams

### 3.2. Effect of Bonding Condition and Joint Type

Bonding condition between the tendon and concrete considerably affected the flexural behavior of the segmental beams with CFRP tendons. The use of bonded tendons greatly increased the strength of the beam as observed in the case of Beams BC3 and BC4 while the use of unbonded tendons greatly improved the deflection capacity of the beams as seen in Beams BC1 and BC2. Bonding condition had no effect on the initial stiffness of the epoxied-joint beams but considerably affected the beams' stiffness after the joint opened as observed in

the load-deflection curves of Beams BC2 and BC4. The failure modes of the beams were also affected by the bonding condition of the tendons as discussed previously. The use of unbonded tendons shifted the failure mode from tension controlled (as observed in Beams BC3 and BC4) to compression controlled (as observed in Beams BC1 and BC2). In Beams BC1 and BC2, severe concrete crushed was observed on the compression zone before the rupture of the CFRP tendons at the ultimate stage.

By comparing the load-deflection curves of Beams BC1 versus BC2 and Beams BC3 versus BC4, it can be observed that regardless of the tendon bonding condition, the type of joints had only a slight effect on the overall load-carrying capacity and ductility of the beams. Both Beams C1 and C2 had similar strength and deflection at the ultimate stage as seen in Figure 3 and that was also true for the cases of Beams C3 and C4, although the beams with epoxied joints showed a bit higher ultimate strength than those with dry joints (Table 2). The joint type had an insignificant effect on the opening of joints. As can be seen from Figure 4, Beams BC1/BC2 and BC3/BC4 showed almost similar load-joint opening curves under the applied load.

## 4. NUMERICAL MODEL

### 4.1 Description of numerical model

This part describes the use of ABAQUS CAE (2012) software to simulate the behaviour of segmental concrete beams internally prestressed with unbonded tendons. To simulate the beams, three-dimensional solid finite elements are used to capture the response of the different components in the finite element models. Eight-node linear brick, reduced integration hexahedral elements (C3D8R) are selected to model the concrete elements, prestressing steel tendons, and auxiliary elements such as steel loading plates, anchor blocks and steel plates at beams' ends. Two-node linear 3-D truss elements are selected to model the conventional steel reinforcement. Details on the material models, contact relationships and modelling procedure are discussed in sequence.

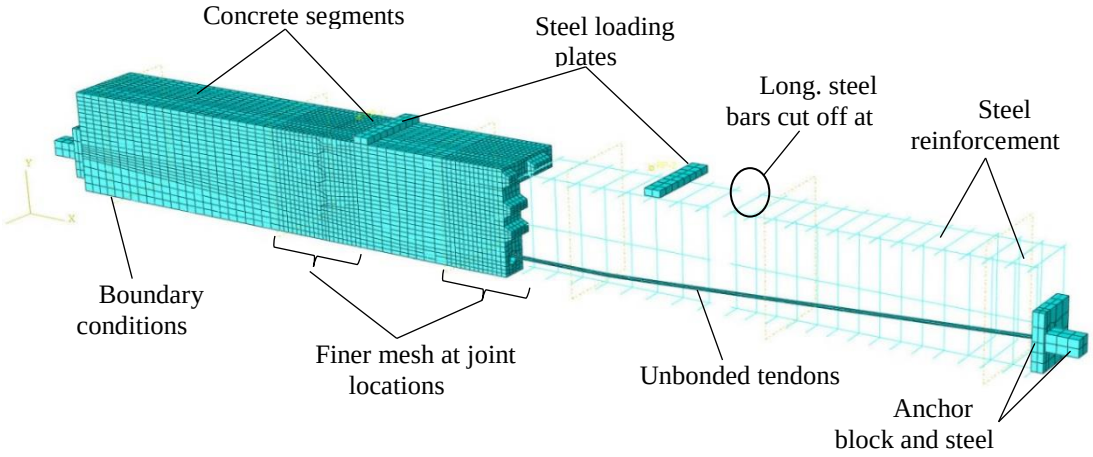


Figure 6. Numerical model

### 4.2. Concrete material model

Concrete damage plasticity (CDP) model which was incorporated in ABAQUS CAE (2012) is used to model concrete elements. The CDP model allows to capture the elastic and plastic behaviour of concrete including damage characteristics in both compression and tension. It can be applied for concrete subjected to static and cyclic loading. Table 3 gives details of CDP parameters used in this study.

The stress-strain curve proposed by Carreira and Chu (1985) is adopted in this study for concrete under compression. The stress-strain relationship for concrete in tension is assumed to consist of a linear ascending part up to the cracking strength $f_{ct}$ and a linear descending part to a total strain of approximately 10 times the strain at the tensile cracking $\varepsilon_{ct}$. The compressive damage parameter $d_c$ and tensile damage parameter $d_t$ proposed by Birtel and Mark (2006) are adopted and integrated in the CDP model for the concrete in compression and tension.

Table 3. Material properties

| Concrete, CDP Parameters | | | | |
|---|---|---|---|---|
| Concrete | | CDP | $\psi$ | 30° |
| Compressive strength (MPa) | 44 | | $e$ | 0.1 |
| Tensile strength (MPa) | 2.65 | | $\sigma_{b0}/\sigma_{c0}$ | 1.16 |
| Elastic modulus $E_c$ (GPa) | 31.17 | | $K_c$ | 0.667 |
| Poisson's ratio | 0.18 | | $\mu$ | 0.001 |
| Steel Reinforcement | | | | |
| | ∅12 | ∅10 | Steel tendons | CFRP tendons |
| Area ($mm^2$) | 113 | 78.5 | 78.5 | 126.7 |
| Elastic modulus $E_c$ (GPa) | 200 | 200 | 195 | 145 |
| Yielding stress (MPa) | 534 | 489 | 1674 | - |
| Ultimate stress (MPa) | 587 | 538 | 1860 | 2450 |
| Poisson's ratio | 0.3 | 0.3 | 0.3 | 0.27 |

### 4.3. Reinforcement material model

An elasto-plastic stress-strain material model is used for conventional steel reinforcements in both tension and compression. The reinforcements including longitudinal and transverse steel bars are embedded into the concrete. For prestressing steel, the stress–strain relationship proposed by Devalapura and Tadros (1992) is adopted in this study. For CFRP tendon, the isotropic elastic material model is chosen to simulate the tendon since CFRP tendon exhibits a linear stress-strain relationship up to the failure. The failure of the CFRP tendons is considered to occur when it reaches its nominal tensile strength $f_{pu}$ (2450 MPa) or when the shear stress in the tendon obtained from the simulation result exceeds its nominal shear resistance, which is equal to 126 MPa as reported in the previous studies (Le et al. 2018; Le et al. 2019).

### 4.4. Modelling procedure

The surface-to-surface contact model incorporated in Abaqus (2012) is chosen to formulate the contacts between joint surfaces of the two adjacent segments (key-key contact), and the contacts between the unbonded tendons and the surrounding concrete (unbonded tendon-concrete contact). For the key-key contact, a friction coefficient of 0.7 is used for the tangential behaviour while hard contact type is used to define the normal behaviour. For the unbonded tendon-concrete contact, frictionless contact type is used for the tangential behaviour while hard contact type is again used for the normal behaviour. Tie constraint contact type is used to model the contacts of steel loading plates to concrete, anchor blocks to end steel plates, and end steel plates to concrete.

The beam model is built symmetrically with regard to the XY plane at the centroid of the beam's cross-section (Figure 5). For the concrete elements, the most critical areas were at joint locations where the cracks happened as observed from the experiment. As such, a finer mesh

with element size of 20 mm is applied for these areas while element size of 40 mm is used for the other areas. The prestressing tendons and the conventional steel reinforcement are meshed with element size of 20 mm. Remaining components are meshed with element size of 40 mm.

The prestressing effects in the model is specified using Predefined Fields function provided in Abaqus (2012). The applied load is exerted by creating two boundary conditions moving vertically downward which are also placed symmetrically at the one-third span length of the beam as shown in Figure 6.

## Model Calibration

Numerical results are validated against the experimental results in terms of the load-deflection response and the failure modes. As observed from Fig. 7, the numerical models well capture the load-deflection responses of the tested beams BS1 and BC1. For Beams BS1 with steel tendons, the test was stopped for the safety reason. At that point, the applied load was 96 kN and its corresponding mid-span deflection was 89.4 mm. In the numerical model, the applied load corresponding to the deflection of 89.4 mm is 91 kN, which deviates approximately -5.7% compared to the experimental result. In the case of Beam BC1 with CFRP tendons, the numerical model slightly overestimates the applied load by 1.8% compared to the experimental result.

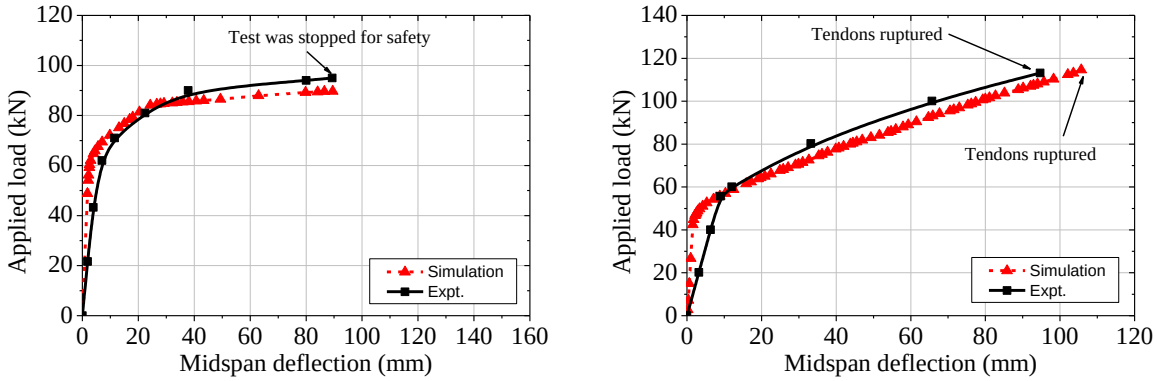


(a) Beam S1 (b) Beam C1

Figure 7. Load-deflection curve: simulation vs experiment. Note: The curve of Beam BS1 is plotted to 89.4 mm deflection, which is equal to expt. value for comparison purpose

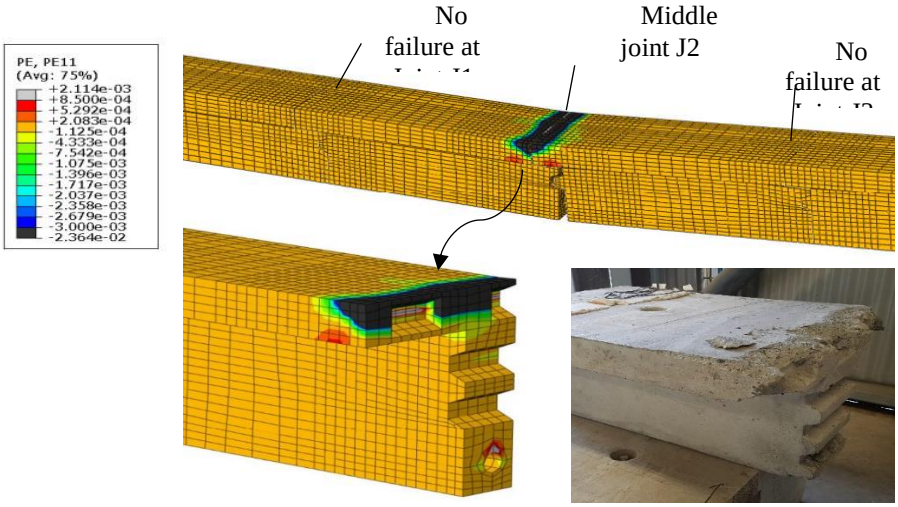


Figure 8. Failure mode of Beam BS1: Simulation vs experiment

The numerical models also well capture the failure modes of the tested beams. The numerical model draws similar failure modes of concrete compared to the tested beams. Only the failure

mode of Beam S1 is provided in Fig. 8 for brevity since both the beams BS1 and BC2 showed similar responses of concrete up to the ultimate stage as discussed above. It is worth noting that the yielding of the prestressing steel takes place before the crushing of the concrete as observed in the numerical model which was very difficult to determine accurately during the test. In the case of Beam BC1, the rupture of the CFRP tendons is also captured in the numerical model near the middle joint J2, which is similar to the test. It is noted from the numerical model that the rupture of the CFRP tendons is due to the shear stress generated in the tendons by the applied load, which exceeds its nominal shear resistance, which could not be measured in the test. From the above discussions, it is evident that the numerical model developed in this study is reliable and entirely capable of simulating the behaviour of PSBs with unbonded tendons of either steel or CFRP material.

## 5. CONCLUSIONS

This study experimentally investigate the use of CFRP tendons on segmental concrete beams. It can be concluded from testing results that CFRP tendons can satisfactory replace the steel tendons for the use in PSBs to tackle the possible corrosion-induced damage in the structure. All the tested beams with bonded/unbonded tendons demonstrated excellent load-carrying and deflection capacities. This study also presents a numerical approach to simulate the flexural behaviour of segmental beams with unbonded tendons. The numerical model is validated against experimental results, therefore is reliable and capable of modelling the behaviour of PSBs with unbonded tendons. This will further support the analysis of segmental beams with unbonded tendons, especially when the CFRP tendon is used in the structure, for which it still requires extensive investigations before applying it to practice.

## ACKNOWLEDGEMENTS

The author acknowledge the financial support from the Australian Research Council Laureate Fellowships FL180100196.

## REFERENCES

ABAQUS CAE (2012). *Analysis user's manual, Version 6.12*, ABAQUS.

Birtel, V., and Mark, P. (2006). "Parameterised finite element modelling of RC beam shear failure." *Proc., ABAQUS Users' Conf.*, 95-108.

Carreira, D. J., and Chu, K.-H. (1985). "Stress-strain relationship for plain concrete in compression." *J. Proc.*, 82(6), 797-804.

Concrete Society Technical Report (2002). "Durable post-tensioned concrete structures." *TR 72*,.

Devalapura, R. K., and Tadros, M. K. (1992). "Stress-strain modeling of 270 ksi low-relaxation prestressing strands." *PCI J.*, 37(2), 100-105.

Le, T. D., Pham, T. M., Hao, H., and Hao, Y. (2018). "Flexural behaviour of precast segmental concrete beams internally prestressed with unbonded CFRP tendons under four-point loading." *Eng. Struct.*, 168(2018), 371-383.

Le, T. D., Pham, T. M., Hao, H., and Yuan, C. (2019). "Performance of precast segmental concrete beams posttensioned with carbon fiber-reinforced polymer (CFRP) tendons." *Compos. Struct.*, 208, 56-69.